

A Circuit-Formulation for the Non-Retarded Maxwell Equations

K.J. van der Kolk and N.P. van der Meijs

Delft University of Technology

Department of EEMCS

Delft, The Netherlands

Email: keesjan@cas.et.tudelft.nl

Abstract—Layout-to-circuit extractors are used by IC designers to determine the physical behavior of a design before it is sent to fabrication. With increasing clock-speeds and decreasing feature sizes, the extraction of circuit models becomes more and more challenging. In this paper we propose a method for extracting RLC circuit-models based on the non-retarded Maxwell equations.

I. INTRODUCTION

Layout-to-circuit extractors are tools used by IC designers to obtain electrical simulation models of integrated circuit designs before tape-out, so that the typical design-cycle can be both fast and economically efficient. However, increasing on-chip frequencies and decreasing feature-sizes are constantly demanding more advanced extraction techniques. Where traditionally extractors have been producing adequate models in the form of RC circuits, nowadays also the modeling of inductive effects is becoming a strong requirement. This is especially true for analog RF circuits, where the exact modeling of integrated passive inductors is a necessity. Further, as is also the case in the digital world, designers are plagued by parasitic inductive effects, such as the skin-effect, substrate eddy-currents, and return-path current-crowding.

We propose a methodology for producing equivalent circuit models from layout, where only resistors, capacitors and inductors are used. The models describe the so-called non-retarded Maxwell equations, which are a simplification of the general Maxwell equations. The non-retarded equations are valid for electromagnetic couplings which extend over areas which are small compared to the wavelength. Inductors are described using the so-called K description [1], which has the desired property that only local couplings need to be accounted for. The resulting models are passive and thus stable, and can be simulated by a modern circuit-simulator.

An advantage of our methodology is that it allows the electromagnetic domain to be split into subdomains, so that each subdomain can be modeled separately. This is convenient, for example, for modeling the interface between inactive and active parts of the chip, since both sides of the interface may require fundamentally different modeling approaches.

II. RELATED WORK

We briefly give a description of related work. Since the literature on extraction of compact IC design models is so

vast, we will point to some key papers which will aid in the understanding of this paper.

In the field of electromagnetic modeling, there exist generally two main approaches, namely the finite element method (FEM) [2], which discretizes the domain of interest into three-dimensional subvolumes, and the boundary element method (BEM) [3], which models only the interactions between the parts of the domain on which charge can accumulate and current is allowed to flow (usually only the surfaces are modeled).

For extracting simulation models from VLSI designs, the BEM modeling technique has been used extensively. One of the reasons is that the discretization is algorithmically simpler, since the space between the conducting bodies need not be discretized in principle. Another reason is that the BEM can exploit a special property that exists generally in VLSI designs, namely that the dielectric media and the substrate doping profile is stratified [4]. Further, in contrast with the FEM, the BEM is able to model the surrounding space of the design without any additional effort.

Volume-based approaches such as the FEM also have their advantages. One important advantage of the FEM is that it allows one to divide the computational domain into logical subdomains, and model each of the subdomains separately. While this is also possible with the BEM, this certainly needs more effort, and doing this may eliminate some of the advantages of the BEM.

If we look at the computational complexity, we find that under certain circumstances, the use of the FEM is advantageous. We note that in VLSI designs, there are many features which are densely packed together, and we assume that the density is more or less homogeneous. Suppose the number of features is n , then the number of nodes in the FEM discretization can also be assumed to be $\mathcal{O}(n)$, due to this homogeneous density of features. Now the BEM method needs to deal with $\mathcal{O}(n^2)$ couplings between elements, while the FEM only needs to account for $\mathcal{O}(n)$ couplings, since all couplings are local. This is of course an advantage of the FEM, but this reasoning only applies for dense IC designs. We further note that domain-decomposition may also help to reduce the extraction effort, since in typical IC designs, there is much repetition in the layout. Thus, geometries which occur frequently need only be modeled once in a FEM-based approach.

In the literature, much effort has been expended on the reduction of the $\mathcal{O}(n^2)$ complexity of BEM models. A popular approach is the Fast Multipole Method (FMM) [5][6], which does not reduce the number of couplings, but it reduces instead the computational complexity of multiplying the model matrix by a vector, which is the most important operation in e.g. iterative solvers. Another approach utilizes the Schur algorithm, so that only couplings within a certain window need to be considered [7].

As mentioned in the introduction, resistance and capacitance have long been regarded the only important quantities to be produced by a circuit extractor, but nowadays inductive effects are also considered very important. A difficulty is that inductance is not a ‘localized property’, i.e., it is defined between current-loops rather than points. To solve this difficulty, the concept of partial inductance was introduced [8]. The further exploitation of this concept has led to the development of the popular PEEC technique [9]. However, PEEC is inherently a BEM method and thus to be practical it must be accelerated by one of the techniques mentioned above, such as FMM.

A different view on accelerating the inductive computations was provided by [1]. Here, it was observed that capacitive panels in the BEM introduce a kind of *shielding*, meaning that if two panels have a certain capacitive coupling, then placing a third panel between them reduces the coupling. The computation of capacitive couplings is similar to that of inductive couplings, except that it involves a matrix inversion step. This inversion is responsible for the shielding effect. Thus in the work just mentioned, the inductance matrix L is inverted as well, yielding the so-called K matrix, or *reluctance matrix*. We will show in this paper that this K description allows us to perform domain-decomposition naturally.

In this paper, we start with the viewpoint of the BEM and use related concepts such as partial inductance and \mathbf{K} couplings. By using domain-decomposition, we divide the domain into small cells, so that we arrive at a volume-based approach, akin towards the FEM. An inherent advantage of our approach is that it reveals how to couple these volume-based domains with BEM based models.

III. ELECTROMAGNETIC MODELING

As mentioned above, the non-retarded Maxwell equations are a simplification of the Maxwell equations which are valid under certain conditions. In order to provide some more insight into these conditions, we provide a derivation of the non-retarded equations in this section.

A. Full-Wave Regime

The macroscopic Maxwell equations are described by

$$\nabla \times \mathbf{E} = -\frac{\partial \mathbf{B}}{\partial t}, \quad (\text{Faraday's law}) \quad (1)$$

$$\nabla \times \mathbf{H} = \mathbf{J} + \frac{\partial \mathbf{D}}{\partial t}, \quad (\text{generalized Ampere's law}) \quad (2)$$

where in linear media, we have the relations

$$\mathbf{B} = \mu \mathbf{H}, \quad (3)$$

$$\mathbf{D} = \varepsilon \mathbf{E}, \quad (4)$$

$$\mathbf{J} = \sigma \mathbf{E}. \quad (5)$$

In the following, we will initially assume that the material parameters μ , ε , and σ are constant. By applying domain-decomposition (see Section IV), we allow the domain to consist of materials with varying parameters. Taking the divergence of (1) and (2) we find that

$$\nabla \cdot \mathbf{B} = 0, \quad (\text{Gauss's law for magnetics}) \quad (6)$$

$$\nabla \cdot \mathbf{D} = \rho, \quad (\text{Gauss's law}) \quad (7)$$

where the last equation stems from the charge-conservation law

$$\nabla \cdot \mathbf{J} = -\frac{\partial \rho}{\partial t}. \quad (8)$$

Essentially, we can thus either use (7) or (8) to describe the law stating that charge is conserved.

B. Potential Formulation

In order to come to the circuit-formulation, we rewrite the original Maxwell equations into potential form. The derivation is well-known, and it may be performed as follows. First, from (6), it can be derived that we may define \mathbf{B} as the curl of another vector-quantity,

$$\mathbf{B} = \nabla \times \mathbf{A}, \quad (9)$$

where \mathbf{A} is the *magnetic vector-potential*. Plugging this into (1), we have that

$$\nabla \times (\mathbf{E} + s\mathbf{A}) = \mathbf{0}. \quad (10)$$

When the curl of any vector-function is zero, we may write that function as the gradient of a scalar function. Thus, there exists a scalar ϕ such that

$$\mathbf{E} + s\mathbf{A} = -\nabla\phi. \quad (11)$$

The minus sign is used here so that ϕ represents the electric scalar potential. The above equation contains *gauge* freedom, i.e., for any scalar function ψ and any constant *const*, it may be equally well written as

$$\mathbf{E} + s(\mathbf{A} + \nabla\psi) = -\nabla(\phi - s\psi + \text{const}), \quad (12)$$

since ψ and *const* will cancel from the above equation. Put differently, \mathbf{A}' and ϕ' equally satisfy (11) when

$$\mathbf{A}' = \mathbf{A} + \nabla\psi, \quad \text{and} \quad \phi' = \phi - s\psi + \text{const}. \quad (13)$$

Combining (2) with (9) and (11), and using the vector identity

$$\nabla \times \nabla \times \mathbf{A} = \nabla \nabla \cdot \mathbf{A} - \nabla^2 \mathbf{A}, \quad (14)$$

we get

$$\nabla^2 \mathbf{A} - s^2 \mu \varepsilon \mathbf{A} = -\mu \mathbf{J} + \nabla(\nabla \cdot \mathbf{A} + s\mu \varepsilon \phi). \quad (15)$$

The last term may be eliminated by assuming the *Lorenz gauge*. That is, we choose ψ in (12) such that

$$\nabla \cdot \mathbf{A} + s\mu\epsilon\phi = 0. \quad (16)$$

It is possible to show that such ψ can always be found. Equation (15) thus reduces to

$$\nabla^2 \mathbf{A} - s^2\mu\epsilon\mathbf{A} = -\mu\mathbf{J}. \quad (17)$$

By combining (7), (11), and using (16), we have

$$\nabla^2 \phi - s^2\mu\epsilon\phi = -\frac{\rho}{\epsilon}. \quad (18)$$

Both equations (17) and (18) are instances of the scalar Helmholtz wave equation

$$(\nabla^2 + k^2)\phi(\mathbf{r}) = -\zeta(\mathbf{r})/\chi, \quad (19)$$

where (17) actually represents three such equations. Note that

$$k^2 = -s^2/c^2 = \omega^2/c^2, \text{ where } c^2 = 1/\mu\epsilon. \quad (20)$$

A solution to the above equation, given ζ , can be found by using the Green's function technique. The Green's function in this case is the solution $g(\mathbf{r}, \mathbf{r}')$ to the problem

$$(\nabla^2 + k^2)g(\mathbf{r}, \mathbf{r}') = -\delta(\mathbf{r} - \mathbf{r}'). \quad (21)$$

Thus, g is the solution to (19) when ζ is a point-source located at \mathbf{r}' , and $\chi = 1$. The solution to this equation is

$$g(\mathbf{r}, \mathbf{r}') = \frac{e^{-jk|\mathbf{r}-\mathbf{r}'|}}{4\pi|\mathbf{r}-\mathbf{r}'|}, \quad (22)$$

see e.g. [10], Section 1.3.3 for a derivation. Intuitively, the source ζ can be seen as a sum of delta functions, and by superposition, the solution to (19) is given by

$$\phi(\mathbf{r}) = \int_{\mathbf{r}' \in \Omega} \frac{g(\mathbf{r}, \mathbf{r}')}{\chi} \zeta(\mathbf{r}') d\mathbf{r}'. \quad (23)$$

This equation can be discretized, e.g., by the Method of Moments [11]. The resulting linear system is then of the form

$$\phi = \mathbf{G}\zeta, \quad (24)$$

where each element in the vectors ϕ and ζ represents respectively the potential and the source in a subvolume, and \mathbf{G} is a matrix of Green's values, where each value is appropriately integrated over each pair of subvolumes.

C. The Non-Retarded Regime

In (22), we see that the variable k introduces a phase-shift in the Green's function. Since

$$k = \omega/c = 2\pi f/c = 2\pi/\lambda, \quad (25)$$

the magnitude of the phase-shift in (22) is

$$k|\mathbf{r} - \mathbf{r}'| = 2\pi|\mathbf{r} - \mathbf{r}'|/\lambda. \quad (26)$$

From this equation we see that if the distances are small compared to the wave-length λ , then we may ignore the phase-shift (retardation) in the Green's function. Essentially, this means that we can set $k = 0$, and (19) reduces to a Poisson equation. In this case, the Green's matrix \mathbf{G} of (24) can be shown to be real, and positive definite.

D. Incorporating Resistive Effects

We have derived two equations for describing the electromagnetic effects, (17) and (18). The former describes magnetic effects, while the second describes capacitive effects. Note that we set $k = 0$ in both equations, since we ignore retardation, as described above. However, we have not yet described the mechanism of resistivity. Resistivity will ultimately describe the source \mathbf{J} in the r.h.s. of (17). The key to determining this source component is in Ohm's law

$$\mathbf{J} = \sigma\mathbf{E}, \quad (27)$$

and in current continuity, i.e., Equation (8). Ignoring the magnetic part of (11), and combining with (27) and (8), we have

$$\nabla^2 \phi = -I_{\text{in}}/\sigma, \text{ with } I_{\text{in}} = \frac{\partial \rho}{\partial t}. \quad (28)$$

Here, I_{in} is the current injected into the domain per unit volume.

Note that equations (18) and (28) both describe ϕ , but they are not contradictory, since the source term in both equations is zero *inside* the homogeneous domain. Hence inside the domain, both equations reduce to the same Laplace equation $\nabla^2 \phi = 0$.

IV. DOMAIN-DECOMPOSITION

As mentioned, it is often necessary to break down a physical domain into several subdomains, so that each part can be analyzed separately.

The fact that domain-decomposition can be applied is based on the following idea. If the Helmholtz equation (19) holds for a certain subdomain Ω_i , then if we know the potential ϕ on the complete boundary of that subdomain, then the potential ϕ *inside* the domain is described *only* by that boundary potential and by the prescribed potentials and sources *inside* the subdomain. This simply follows from the fact that the Helmholtz equation is a differential equation, i.e., the potential at each point is related to the potentials at (infinitesimally close) *neighboring* points.

As a practical example, if we have a domain Ω which is composed of several materials with different properties, we can decompose that domain into subdomains, where each subdomain has homogeneous properties, and find a model for each of the subdomains. We then link those models together by equating the potentials at the boundaries of those domains. This example shows that domain-decomposition can be used as a tool to save us from the trouble of dealing with inhomogeneous domains.

V. DERIVING A CIRCUIT MODEL

In this section we will take the electromagnetic modeling strategy developed above and find a modeling approach based on circuit-elements.

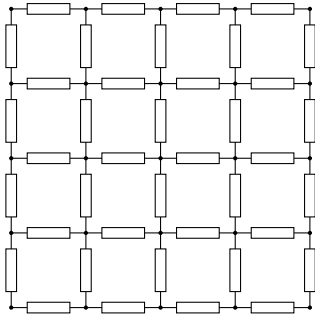


Figure 1: Structured grid of resistors.

A. Resistive and Capacitive Models

First, we find a model for the resistive effects, i.e., Equation (28). If we set $\chi = \sigma$ and $\varsigma = I_{in}$, then this equation is solved by (23), or in the discrete case (24). By renaming variables $\phi \rightarrow \mathbf{v}$, $\varsigma \rightarrow \mathbf{i}$, and defining $\mathbf{Y} \equiv \mathbf{G}^{-1}$, we have

$$\mathbf{Y}\mathbf{v} = \mathbf{i}, \quad (29)$$

where \mathbf{Y} is an admittance matrix and \mathbf{v} and \mathbf{i} are vectors of voltages and currents, respectively.

The above equation can be used in any kind of discretization since it is essentially a boundary-element model. It is well-known that a resistive domain can be modeled by a structured mesh consisting of resistors, as illustrated for two-dimensions in Figure 1. Here, each resistor represents a filament through which current is allowed to flow. By domain-decomposition, each node has only couplings to neighboring nodes. The admittance between two nodes is given by

$$Y = \frac{\sigma S}{d}, \quad (30)$$

where S is the cross-sectional area of the filament, and d is the length of the filament.

In the following, we will use the model (30) based on the structured-mesh instead of the BEM-based model given by (29). However, we keep the BEM-based model for reference, and use it to derive the inductive model in the next subsection by analogy.

Note that in the structured mesh, filaments in orthogonal directions will overlap, while filaments in equal directions may not. We can see in the figure that the ‘averaging’ effect of the potential by the Laplace operator is implemented by resistors, while the source of the Poisson equation may be implemented by injecting currents into the nodes at the boundary.

For the capacitive model, we take (18), with $k = 0$, and thus $\chi = \varepsilon$ and $\varsigma = \rho$. Taking (24) and renaming variables $\phi \rightarrow \mathbf{v}$, $\varsigma \rightarrow \int \mathbf{i} dt$ (charge), and $\mathbf{C} = \mathbf{G}^{-1}$, we obtain

$$\mathbf{s}\mathbf{C}\mathbf{v} = \mathbf{i}, \quad (31)$$

where \mathbf{C} is a capacitance matrix, and \mathbf{v} and \mathbf{i} are voltages and currents, as before.

Like in the resistive case, we can model capacitive effects by a structured mesh of capacitors. As in (30), we can compute

the value of a capacitor on the grid as

$$C = \frac{\varepsilon S}{d}, \quad (32)$$

which is essentially the parallel-plate formula for capacitors.

We should point out that the capacitive model obtained in this way is valid for a finite domain. That is, any capacitive coupling through the exterior of the domain is ignored (this is equivalent to assuming that $\varepsilon = 0$ outside the domain). One way to deal with this problem is to apply a boundary element method to the surface of the domain, but this is outside the scope of this paper. Another strategy may be to simply ignore those couplings, since they might turn out to be insignificant in a particular application.

B. Inductive Model

Now we model the inductive effects. First we recall that the relevant equation, (17), is actually composed of three equations. To handle the vectorial nature of the equation, we write

$$\hat{\mathbf{a}} = \mathbf{G}\hat{\mathbf{i}} \quad (33)$$

where $\hat{\mathbf{a}}$ and $\hat{\mathbf{i}}$ are both $N \times 3$, where N is the number of subvolumes. Each row of $\hat{\mathbf{a}}$ represents the (average) vector potential in a filament as projected onto the three coordinate axes. Each row of $\hat{\mathbf{i}}$ represents the (average) directional current in the corresponding filament, multiplied by the length of the filament, i.e.,

$$\hat{\mathbf{i}}[m, \star] = I_m h_m \mathbf{x}_m^T, \quad (34)$$

where \mathbf{x}_m is a unit vector pointing into the direction of the filament, I_m is the current through the filament, and h_m is the length of the filament.

In order to relate the magnetic vector potentials to the induced voltages in each filament, we will use (11), where we note that the magnetic contribution to the electric field comes from the term $s\mathbf{A}$. Integrating this term along the length of the filament gives us the induced voltage in filament m ,

$$v_m = s \int \mathbf{A}_m \cdot d\mathbf{h}_m, \text{ or } v_m = s h_m \hat{\mathbf{a}}[m, \star] \cdot \mathbf{x}_m^T. \quad (35)$$

Now, by some algebraic manipulation, we can write (33) as

$$\mathbf{v}_{\text{branch}} = s\mathbf{L}\mathbf{i}, \quad (36)$$

i.e., the magnetic effects are modeled by an *inductance matrix*, with elements

$$l_{ij} = g_{ij} h_i h_j (\mathbf{x}_i^T \cdot \mathbf{x}_j). \quad (37)$$

In the previous subsection, we derived a resistive and capacitive model for a structured mesh. We would like to do the same for the inductive effects, and we proceed as follows. First, we assume that the filaments are oriented along the coordinate axes. In that case, $\mathbf{x}_i^T \cdot \mathbf{x}_j$ is either 0 or 1. Hence, the problem is completely decoupled in the three orthogonal directions, and we will assume now briefly that all filaments

are oriented along the x -axis. Equation (37) can then be written as

$$\mathbf{L} = \mathbf{H}\mathbf{G}\mathbf{H} \quad (38)$$

where \mathbf{H} is a diagonal matrix in which entry i is equal to the length h_i of filament i . Now, recall from the previous subsection that the admittance and capacitance matrices are obtained by inverting the Green's matrix \mathbf{G} . To obtain a similar modeling approach for inductances, we define $\mathbf{K} = \mathbf{L}^{-1}$, following [1].

Now, by analogy, we can define the coupling between two neighboring filaments in a structured mesh by the parallel-plate formula

$$K = \frac{S}{\mu d h_i h_j}, \quad (39)$$

where h_i and h_j are the lengths of the abutting filaments (these lengths are usually equal), S is the area of contact between the two filaments, and d is the distance between the centers of the filaments. Note that μ appears in the denominator, since by comparing (17) and (19), we have $\chi = 1/\mu$.

C. Illustrative Comparison of Resistive and Inductive Models

The resistive network obtained in Subsection V-A implements the 'averaging' behavior of the Laplace equation, which we will explain now. Consider a source-free region Ω , and within it a ball Ω_S with radius r , and assume that the origin is at the center of the ball. Assume that the Laplace equation $\nabla^2 \phi = 0$ holds, then integrating over the ball, and using the divergence theorem, we have that

$$\int_{\Omega_S} \nabla^2 \phi dV = \int_{\partial\Omega_S} (\nabla \phi) \cdot dS \quad (40)$$

$$= \int_{\partial\Omega_S} \frac{\partial \phi}{\partial r} dS \quad (41)$$

$$= 0 \quad (42)$$

Now integrating this for increasing radius of the ball,

$$\int_0^R \int_{\partial\Omega_S} \frac{\partial \phi}{\partial r} dS dr = \int_{\partial\Omega_S} \int_0^R \frac{\partial \phi}{\partial r} dr dS \quad (43)$$

$$= \int_{\partial\Omega_S} [\phi(R) - \phi(0)] dS \quad (44)$$

$$= \int_{\partial\Omega_S} \phi(R) dS - 4\pi R^2 \phi(0) \quad (45)$$

$$= 0, \quad (46)$$

or

$$\phi(0) = \frac{1}{4\pi R^2} \int_{\partial\Omega_S} \phi(R) dS, \quad (47)$$

which shows that indeed the potential at the center of the ball is equal to the average of the potential at the surface of the ball, for a source-free region.

Consider now Figure 2, which illustrates part of the structured grid, in a two-dimensional configuration. If the conductances are all equal to Y , then the potential at the center node

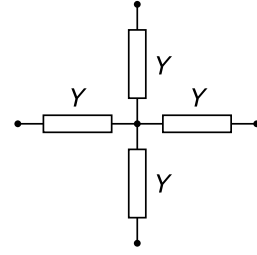


Figure 2: Resistive 4-way star network.

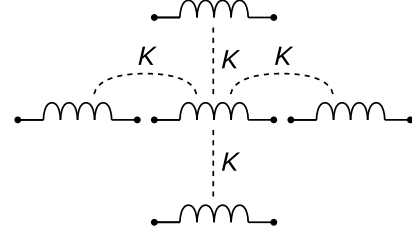


Figure 3: Inductive 4-way star network.

is equal to the average of the potentials at the outer nodes. For illustration, we write down the MNA-formulation of this model,

$$\mathbf{i} = \begin{bmatrix} 4Y & -Y & -Y & -Y & -Y \\ -Y & Y & 0 & 0 & 0 \\ -Y & 0 & Y & 0 & 0 \\ -Y & 0 & 0 & Y & 0 \\ -Y & 0 & 0 & 0 & Y \end{bmatrix} \mathbf{v}, \quad (48)$$

where the first row and column correspond to the center node. Indeed, this model shows that the potential at the center is $1/4$ of the sum of the other potentials, if the current injected into the center node is zero.

Consider now Figure 3. Here, the inductances are coupled by a K -coupling of magnitude K . The corresponding circuit equation is

$$\mathbf{s}\mathbf{i}_{\text{branch}} = \begin{bmatrix} 4K & -K & -K & -K & -K \\ -K & K & 0 & 0 & 0 \\ -K & 0 & K & 0 & 0 \\ -K & 0 & 0 & K & 0 \\ -K & 0 & 0 & 0 & K \end{bmatrix} \mathbf{v}_{\text{branch}}, \quad (49)$$

Apart from the fact that branch-potentials and branch-currents are used, the model is completely analogous to the resistive case. This illustrates that the inductive model equally well solves the Laplace equation. If external sources are applied, then the models are also analogous. Note that an injected current in the resistive case corresponds to an injected branch-current in the inductive case.

D. Elementary Branch Circuit

In this subsection, we will bring the resistive, capacitive and inductive models together to form the circuit model. To do this, we divide the domain into a structured mesh, and describe the

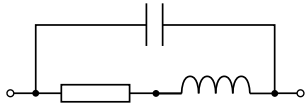


Figure 4: Elementary branch circuit.

relation between the potentials at the nodes of the grid, and the currents along the edges of the grid.

From Equation (11) and Ohm’s law (27), we see that the current along an edge can be discretized by a resistor and an inductor in series; recall from (35) how the vector potential in a filament translates to an inductor branch-voltage. Further, we have that (18) holds, meaning that between the nodes in the grid we need to place capacitances, as outlined in Subsection V-A.

Hence, the *elementary branch circuit* that is to be placed between two nodes on the grid is shown in Figure 4. Here, the inductive couplings between abutting filaments is not shown of course, since there is only one inductor in the figure, but one should be aware that these couplings exist.

When assembling the branch circuits into a larger circuit, only couplings exist between neighboring elements. That is, no long-range couplings exist. Hence if there are N nodes in the domain, then only $\mathcal{O}(N)$ couplings exist.

E. Domain-Decomposition on Circuits

In the previous subsection, we showed how a circuit model can be obtained. Essentially, for each cube in the grid, we have 12 edges, on which an elementary branch circuit is placed. It seems natural that the model can be subdivided into submodels by ‘cutting’ the circuit at the nodes. A problem, however, is that the filaments have inductive couplings between each other, which we would also need to cut.

Instead of cutting inductive couplings, recall from (35) that the vector potential in a filament can be translated to a vector-potential, and vice versa. Hence, on the boundary between two subdomains, we can introduce two *dummy inductors*, which have the purpose of transmitting the vector potential from one subdomain to the other. In principle, a dummy inductor can be regarded as a two-dimensional filament, which is placed against the cube cell. Two of these filaments will meet at an interface, and we connect both ends of the corresponding inductors to each other. In order to keep the node potentials well-defined, we ground one of the nodes (this is necessary, because the vector-potential translates to a branch-voltage, not an absolute potential).

VI. AN EXAMPLE

As an example, we will model a microstrip transmission-line structure and compare the impedance function in the frequency domain with a standard textbook model. The parameters are as follows:

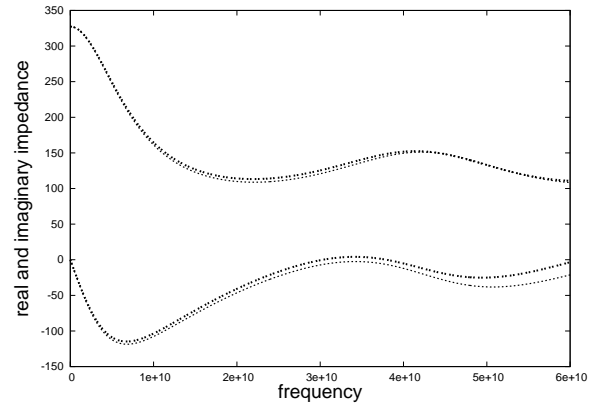


Figure 5: Simulation of the impedance of a microstrip, and comparison with textbook solution.

length	1800 μm
width	10 μm
thickness	10 μm
conductor thickness	0.05 μm
conductivity	$37.71 \cdot 10^6 \text{ S/m}$ (aluminum)
terminating resistance	200 Ω

Note that the strip is much larger than the smallest wavelength, but since the wave is trapped between the strips, there are no long-range effects. In our model, we used 40 blocks to model each strip, and 40 blocks to model the space between the strips. The exterior capacitive and inductive effects are ignored (no BEM model was attached to the structure).

The textbook solution was found by making a 20-stage transmission line RLC model, and simulating it using SPICE. The real and imaginary parts of the simulation are shown in Figure 5. The textbook solution is also shown.

VII. CONCLUSION

We have presented a method for generating RLC circuit models for electromagnetic problems. We have shown how the use of the K -method enables domain-decomposition, so that the problem domain can be elegantly divided into subdomains. An example illustrates the validity of the method.

REFERENCES

- [1] A. Devgan, H. Ji, and W. Dai, “How to efficiently capture on-chip inductance effects: Introducing a new circuit element k ,” in *ICCAD ’00: Proceedings of the Int. Conf. on Computer-Aided Design*, November 2000, pp. 150–155.
- [2] P. P. Silvester and R. L. Ferrari, *Finite Elements for Electrical Engineers*. Cambridge University Press, 1996.
- [3] P. K. Banerjee, *The Boundary Element Methods in Engineering*. McGraw-Hill College, 1994.
- [4] T. Smedes, N. P. van der Meijs, and A. van Genderen, “Boundary element methods for capacitance and substrate resistance calculations in a vlsi layout verification package,” in *Proc. International Conf. on Software for*

- Elect. Eng. Analysis and Design*, July 1993, pp. 337–344.
- [5] L. Greengard and V. Rokhlin, “A fast algorithm for particle simulations,” *J. Comput. Phys.*, vol. 73, no. 2, pp. 325–348, 1987.
 - [6] M. Kamon, M. Ttsuk, and J. White, “Fasthenry: a multipole-accelerated 3-d inductance extraction,” vol. 42, pp. 1750–1758, 1994.
 - [7] N. P. van der Meijs and A. J. van Genderen, “An efficient finite element method for submicron ic capacitance extraction,” in *DAC '89: Proceedings of the 26th ACM/IEEE conference on Design automation*. New York, NY, USA: ACM, 1989, pp. 678–681.
 - [8] A. Ruehli, “Inductance calculations in a complex integrated circuit environment,” *IBM Journal of Research and Development*, no. 5, pp. 470–481, September 1972.
 - [9] —, “Equivalent circuit models for three-dimensional multiconductor systems,” *Microwave Theory and Techniques, IEEE Transactions on*, vol. 22, no. 3, pp. 216–221, Mar 1974.
 - [10] G. W. Hanson and A. B. Yakovlev, *Operator Theory for Electromagnetics : An Introduction*. New York: Springer-Verlag, 2002.
 - [11] R. F. Harrington, *Field Computation by Moment Methods*. Wiley-IEEE Press, 1993.